AFRL-AFOSR-VA-TR-2019-0196

Rational Design of Mechanical Properties of Polacrylonitrile Carbon Fibers from the Nanoscale

Satish Kumar
GEORGIA TECH RESEARCH CORPORATION

10/05/2018
Final Report

Air Force Research Laboratory
AF Office Of Scientific Research (AFOSR)/ RTA1
Arlington, Virginia 22203
Air Force Materiel Command

REPORT DOCUMENTATION PAGE

Form Approved
OMB No. 0704-0188

1. REPORT DATE *(DD-MM-YYYY)*	**2. REPORT TYPE**	**3. DATES COVERED** *(From - To)*
09/17/2018	Final	07/15/2014 - 07/14/2018

4. TITLE AND SUBTITLE
Rational Design of Mechanical Properties of Polyacrylonitrile Carbon Fibers

5a. CONTRACT NUMBER

5b. GRANT NUMBER
FA9550-14-1-0194

5c. PROGRAM ELEMENT NUMBER

6. AUTHOR(S)
Satish Kumar and Hendrik Heinz

5d. PROJECT NUMBER

5e. TASK NUMBER

5f. WORK UNIT NUMBER

7. PERFORMING ORGANIZATION NAME(S) AND ADDRESS(ES)
Georgia Institute of Technology
University of Colorado, Boulder

8. PERFORMING ORGANIZATION REPORT NUMBER

9. SPONSORING/MONITORING AGENCY NAME(S) AND ADDRESS(ES)
AFOSR/RTA
875 N. Randolph Street
Arlington VA 22203-1768

10. SPONSOR/MONITOR'S ACRONYM(S)
AFOSR

11. SPONSOR/MONITOR'S REPORT NUMBER(S)

12. DISTRIBUTION/AVAILABILITY STATEMENT

13. SUPPLEMENTARY NOTES

14. ABSTRACT

Research efforts reported here include the following: (i) To manufacture high strength (>5.5 GPa) high modulus (>350 GPa) carbon fibers from polyacrylonitrile (PAN) copolymers. (ii) To manufacture low density hollow carbon fibers. (iii) To reduce energy used in carbon fiber manufacturing. (iv) To manufacture carbon fibers from PAN/cellulose nano crystals (CNC) and PAN/lignin blends. (v) To manufacture PAN/BNNT based carbon fibers. Modeling studies have been used to provide guidance to this effort. Results of these studies are summarized and documented in this report. In addition, the results that have implications beyond carbon fiber manufacturing are also presented.

15. SUBJECT TERMS
Polyacrylonitrile, carbon nanotubes, carbon fibers, cellulose nano crystals, lignin

16. SECURITY CLASSIFICATION OF:			**17. LIMITATION OF ABSTRACT**	**18. NUMBER OF PAGES**	**19a. NAME OF RESPONSIBLE PERSON**
a. REPORT	**b. ABSTRACT**	**c. THIS PAGE**		25	**19b. TELEPHONE NUMBER** *(Include area code)*

Rational Design of Mechanical Properties of Polyacrylonitrile Carbon Fibers from the Nanoscale

Satish Kumar (Satish.kumar@mse.gatech.edu)

Hendrik Heinz (Hendrik.heinz@colorado.edu)

FA9550-14-1-0194

Table of contents

Abstract

Research efforts reported here include the following: (i) To manufacture high strength (>5.5 GPa) high modulus (>350 GPa) carbon fibers from polyacrylonitrile (PAN) copolymers. (ii) To manufacture low density hollow carbon fibers. (iii) To reduce energy used in carbon fiber manufacturing. (iv) To manufacture carbon fibers from PAN/cellulose nano crystals (CNC) and PAN/lignin blends. (v) To manufacture PAN/BNNT based carbon fibers. Modeling studies have been used to provide guidance to this effort. Results of these studies are summarized and documented in this report. In addition, the results that have implications beyond carbon fiber manufacturing are also presented.

Results of this study are documented in 32 publications and 6 Ph.D. theses. These publications and theses are included as part of this report by reference. Results of some of the published studies are also summarized here. Unpublished work is discussed in somewhat more detail.

SECTION I – Summary

High Strength and High Modulus Carbon Fibers (Publication #4, 5, 6, 7, 8, 11, 14, 23, and 32):

Carbon fibers have been processed from gel spun polyacrylonitrile copolymer on a continuous carbonization line with a tensile strength in the range of 5.5 to 5.8 GPa, and tensile modulus in the range of 354 to 375 GPa. **This combination of strength and modulus is the highest for any continuous fiber reported to date, and the gel spinning route provides a pathway for further improvements in strength and modulus for mass production of carbon fibers. At short gauge length, fiber tensile strength was as high as 12.1 GPa, which is amongst the highest values reported for a PAN based carbon fiber.** Structure analysis shows random flaws of about 2 nm size, which results in intrinsic tensile strength of higher than 20 GPa. Inter-planar turbostratic graphite shear modulus in high strength carbon fibers is 30 GPa, while in graphite the corresponding value is only 4 GPa.

By gel spinning of islands-in-the-sea bi-component fibers, progress has been made in making small diameter carbon fiber (effective diameter about 2.5 μm) from PAN with a modulus value as high as 400 GPa. Based on the data extrapolation, it is predicted that PAN based carbon fibers with a diameter of 1 μm will have a tensile strength of 12 GPa and tensile modulus of >420 GPa.

Effect of solution homogeneity on carbon fiber properties has been examined. Poly(acrylonitrile-co-methacrylic acid) (PAN-co-MAA)/N,N dimethylformamide (DMF) solutions were prepared and dynamic shear rheology of these solutions were investigated. With increasing stirring time up to 72 h at 70 °C, the polymer solution became less elastic (more liquid-like) with a 60% reduction in the zero-shear viscosity. Relaxation spectra of the PAN-co-MAA/DMF solutions yield a decrease in relaxation time, corresponding to an about 8% decrease in viscosity average molecular weight. The log-log plot of G' (storage modulus) versus G" (loss modulus) exhibited an increase in slope as a function of stirring time, suggesting that the molecular level solution homogeneity increased. In order to study the effect of solution homogeneity on the resulting carbon fiber tensile strength, multiple PAN-co-MAA/DMF solutions were prepared, and the precursor fibers were processed using gel-spinning, followed by continuous stabilization and carbonization. The

rheological properties of each solution were also measured and correlated with the tensile strength values of the carbon fibers. It was observed that with increasing the slope of the G' versus G" log-log plot from 1.471 to 1.552, and reducing inter-filament fiber friction during precursor fiber drawing through the addition of a fiber washing step prior to fiber drawing, the carbon fiber strength was improved (from 3.7 to 5.8 GPa). This suggests that along with precursor fiber manufacturing and carbonization, the solution homogeneity is also very important to obtain high strength carbon fiber.

The addition of 1 wt% CNT in the gel spun PAN precursor fiber results in carbon fibers with 68% higher thermal conductivity when compared to the control gel spun PAN based carbon fiber, and a 103% and 146% increase over commercially available IM7 and T300 carbon fibers, respectively. The electrical conductivity of the gel spun PAN/CNT based carbon fibers also showed improvement over the investigated commercially available carbon fibers. Increases in thermal and electrical conductivities are attributed to the formation of the highly ordered graphitic structure observed in the high resolution transmission electron microscopy images.

Polyacrylonitrile (PAN) and PAN/carbon nanotube (PAN/CNT) fibers were manufactured through dry-jet wet spinning and gel spinning. Fiber coagulation occurred in a solvent-free or solvent/non-solvent coagulation bath mixture with temperatures ranging from -50 °C to 25 °C. The effect of fiber processing conditions was studied to understand their effect on the as-spun fiber cross-sectional shape, as well as the as-spun fiber morphology. Increased coagulation bath temperature and a higher concentration of solvent in the coagulation bath medium resulted in more circular fibers and smoother fiber surface. As-spun fibers were then drawn to investigate the relationship between as-spun fiber processing conditions and the drawn precursor fiber structure and mechanical properties.

Fiber spinning, stabilization, and carbonization studies that build on the above studies should result in further increase in fiber tensile properties.

Low Energy Carbon Fiber Manufacturing (Publication #1)

Carbon Nanotube (CNT) can exhibit electrical conductivity and introduce electric current into polymer. Using dry-jet-wet spin technology, polyacrylonitrile (PAN)/CNT composite fibers with 15 wt% and 20 wt% of CNT content were fabricated. The electrical conductivity of PAN/CNT fibers was enhanced by the annealing process at different temperatures and changed with time. These fibers could also respond to stretching, and the electrical conductivity decreased by 50 % when the elongation reached 3%. In addition, electrical current can induce Joule heating effect and thermally transform PAN/CNT composite fibers. With the application of various electrical currents up to 7 mA at a fixed length, conductivity was enhanced from around 25 S/m to higher than 800 S/m, and composite fibers were stabilized in air. On application of electric current, the temperature of composite fibers can increase from room temperature to hundreds of degree Celsius measured by an infra-red (IR) microscope. Joule heating effect can also be estimated according to one-dimensional steady-state heat transfer equation, which reveals the temperature can be high enough to stabilize or carbonize fibers. As a result, **this research provides a new idea of heating fabrics for thermal regulation, and a new approach for stabilizing and carbonizing PAN**

based carbon fibers. Using this approach, it should be possible to manufacture carbon fibers using significantly lower energy than the approach currently industrially practiced.

Low Density Hollow Carbon Fiber (Publication #2, 3, and 12)

Sheath-core polyacrylonitrile (PAN)/poly(methyl methacrylate) fibers were spun through bi-component dry-jet gel-spinning method, and were used for fabricating hollow carbon fibers. After optimizing stabilization and carbonization conditions, the resulting PAN based hollow carbon fibers, manufactured using batch stabilization and carbonization, possessed an average strength and modulus of 3.16 GPa and 275 GPa, respectively. Additionally, 1 wt% carbon nanotubes was added to PAN portion to form PAN+CNT sheath. The PAN+CNT based hollow carbon fiber had an average strength of 3.24 GPa and modulus of 254 GPa. **These hollow carbon fibers can be used for fabricating low density and high performance structural composite materials**.

Graphene oxide nanoribbon (GONR) made by the oxidative unzipping of multiwalled carbon nanotubes (MWCNTs) were dispersed in dimethylformamide (DMF) and mixed with polyacrylonitrile (PAN) to fabricate continuous PAN/GONR composite fibers by gel spinning. Subsequently, PAN/GONR composite fibers were stabilized and carbonized in batch process to fabricate composite carbon fibers. Structure, processing and properties of the composite precursor and carbon fibers have been studied. **This study shows that GONR can be used to make porous (and hence low density) precursor and carbon fibers**. In addition, GONR also shows the potential to make higher mechanical property carbon fibers than that achieved from PAN precursor only.

PAN/CNC nano composite fibers and carbon fibers (Publication #9, 16, 21, 26, and 29)

Polyacrylonitrile (PAN)/cellulose nano crystal (CNC) fibers containing 0, 1, 5, 10, 20, and 40 wt % CNCs have been successfully produced by gel spinning. The rheological properties of solutions were investigated and the results showed that the complex viscosity and storage modulus of solutions were significantly affected by the presence of CNCs in the solution. Structure, morphology, mechanical properties and dynamic mechanical properties of these fibers have been investigated.

Good dispersion of cellulose nanocrystals (CNCs) in the polymer matrix is one of the key factors to obtaining good properties in the resulting nano composites. However, the preparation of individually dispersed CNCs in solvents or in polymer matrices has been a challenge. In this study, individually dispersed wood-based CNCs have been successfully prepared in solvents, including dimethyl formamide (DMF), H_2O, and a mixture of H_2O/DMF, by sonication of moisture-containing CNCs. The CNCs dispersions were characterized by dynamic light scattering (DLS). It is found that CNCs containing above about 3.8 wt % moisture is critical for achieving individually dispersed CNC in solvents. Hydrodynamic radius (Rh) of CNCs is smaller in H_2O/DMF co-solvent mixture than that in pure DMF or in pure H_2O under same sonication treatment conditions. Experimental results have been corroborated using molecular simulation study.

To the best of our knowledge, this is the first study that shows that nano composites can be made with as high a filler loading as 40 wt% without loss in strain to failure, or even show increase in strain to failure and toughness, depending on the drawing conditions.

Polyacrylonitrile (PAN) fibers containing up to 40 wt% cellulose nanocrystals (CNC) have been successfully stabilized and carbonized to make carbon fibers. Under the batch process, PAN/CNC based carbon fibers exhibit a tensile strength in the range of 1.8 – 2.3 GPa, and tensile modulus in the range of 220 - 265 GPa, which are comparable to the control PAN-based carbon fibers. Based on the transmission electron microscopy study, individually distributed CNC regions surrounded by PAN matrix were observed in the stabilized and carbonized fibers. Carbonized fibers show clear boundaries between PAN and CNCs based carbon regions. This study shows that biphasic carbon fibers can be made from the PAN/CNC system. Further details on PAN/CNC carbon fibers are included elsewhere in this report. However, to fully explore the PAN/CNC carbon fiber space, further studies are needed, including stabilization and carbonization on a continuous line.

PAN/Lignin blend fibers and carbon fibers (Publications #13, 15, and 22)

Composite fibers comprised of lignin, polyacrylonitrile (PAN), and carbon nanotubes (CNT) were successfully fabricated by gel-spinning technology. PAN, PAN/lignin, and PAN/lignin/CNT precursors have been converted to carbon fibers under identical stabilization and carbonization conditions. PAN/lignin carbon fiber exhibits comparable mechanical properties to PAN carbon fiber. Raman spectroscopy studies suggested differences between the carbon fibers when lignin and CNTs were incorporated.

Thermal stabilization reactions (e.g. oxidation, cyclization, and crosslinking) for both PAN and PAN/soft wool lignin (SWL) fibers were individually studied by different scanning calorimetry. The addition of SWL was shown to reduce the activation energies and increase reaction rates of cyclization, oxidation and crosslinking. Thermo-mechanical analysis (TMA) was employed to monitor the effect of applied tensions on PAN cyclization kinetics under non-isothermal heating process. Cyclization activation energies of PAN/SWL fiber are shown to be consistently lower than those of PAN fiber under all applied tensions. Calculations of cyclization reaction kinetics constants from TMA indicate that SWL can promote PAN cyclization and crosslinking.

PAN sheath and PAN/lignin core bi-component fibers have been made by gel spinning and these bi-component fibers have been carbonized in batch process. It was further shown that PAN sheath carbonized without significant porosity, while PAN/lignin core exhibited significant porosity.

PAN/lignin based carbon fibers are being made to reduce the cost of carbon fibers and to make them more sustainable by increasing their bio-renewable content.

PAN/BNNT fibers and carbon fibers

Polyacrylonitrile (PAN)/boron nitride nanotube (BNNT) composite fibers were spun using gel spinning method and the resulting carbon fibers were processed after the fibers were stabilized in

air and subsequently carbonized in nitrogen. Both stabilization and carbonization were done in batch process. PAN fibers containing 1 wt% BNNTs show comparable drawability to the control PAN fiber while the drawability of composite fibers significantly decreases as BNNT concentration increased to 5 wt%. Differential scanning calorimetry suggests that the presence of BNNTs reduces the activation energy of oxidation and crosslinking reactions but has little effect on the activation energy of cyclization reaction. In the PAN/BNNT based carbon fibers, the graphitic carbon structure that formed in the vicinity of BNNT at 1300°C carbonization temperature was directly observed by transmission electron microscopy. Orientation and interfacial stress transfer in PAN/BNNT fibers were determined by Raman spectroscopy. Further details on this work are included elsewhere in this report.

Carbon films:

In the first experiment of its kind, PAN precursor film has been processed, and stabilized and carbonized. In this first trial carbon film modulus was 200 GPa, with a film thickness of about 3.75 μm, and film width of 0.3 mm.

Other Outcomes: (Publication #10, 17, 20, 25, and 27)

We have discovered the ordered helical wrapping of PMMA on single wall carbon nano tube (SWCNT). PMMA wrapped SWCNT allows, CNT dispersion in PAN (and in many other polymers) as individual carbon nanotubes, rather than a bundle of nanotubes. PMMA wrapped SWCNT also enhance CNT-CNT inter tube stress transfer. As a result bucky papers made from PMMA wrapped SWCNT exhibits six times the modulus of SWCNT bucky paper without PMMA wrapping. PAN fibers have also been made with PMMA wrapped SWCNT, and for comparison with SWCNT without PMMA wrapping. A procedure has also been developed that shows that PMMA wrapped SWCNT bucky papers can exhibit a surface area as high as ~1000 m^2/g. Significantly enhanced performance of such bucky papers as compared to bucky papers processed without PMMA wrapping, in energy storage (electrochemical supercapacitors) has been demonstrated. Interfacial shear strength has been evaluated in select polymer/CNT systems.

Modeling and Simulation Summary (Publication # 18, 19, 28, 30, and 31)

The project lead to quantitative insights into the miscibility of carbon nanofiber precursors in solution and into the interfacial shear strength and glass transition temperatures of a number of CNT/polyacrylonitrile (PAN) composites in all-atom resolution. Solutions of PAN and PMMA in DMSO were found to be a more favorable medium for CNT dispersion than DMF and DMAc. PMMA showed consistently higher binding affinity to CNTs compared to PAN, which is associated with more favorable van-der-Waals interactions and also seen in experiment (publication #4). Mechanical properties of CNT/PAN composites depend on the interfacial area per unit volume and unit mass, and accordingly show higher glass transition temperatures and higher interfacial shear strength. The use of SWCNTs, if well dispersed, is likely to result in better

mechanical properties than the use of MWCNTs. We also analyzed the impact of interphase engineering on the properties of CNT/polymer composites, for example, due to conformation preferences of poly(methyl methacrylate) (PMMA) on CNTs as a function of CNT diameter, chirality, and temperature. We developed and applied new computational models for graphitic materials at the all-atom scale that include virtual π electrons. These new computational models for graphite, graphene, CNTs, and their interfaces achieve more than ten times higher accuracy than prior models in predicting π-π and ion-π interactions, shear stability between graphene layers, surface, and interfacial energies through the inclusion of internal polarity mediated by the π electron cloud at minimal computational cost. The use of the models in this project and the related publications are a new milestone for computationally guided design of carbon nanomaterials and nanofibers. The application of these models extends beyond the scope of this project to many graphitic hybrid material, for example, materials for space exploration (NASA needs), predictions in sensing and molecular recognition using carbon-based substrates (Air Force), and more accurate descriptions of nucleobase interactions in biology (modeling DNA and RNA also depends on the accurate inclusion of π-π and ion-π interactions which is not accounted for in biomolecular force fields).

The results advance the understanding of experimental data and rational design of carbon nanofibers in the Kumar group and by other experimental groups to reduce the number of trial-and-error studies. The early interactions between CNTs and polymer precursors for carbon nanofibers in solution were confirmed to be overall challenging to control as simulations also show that CNTs thermodynamically prefer to bundle in DMSO, DMF, and in DMAc (this also happens in water and other polar solvents). Certain combinations of polymer, solvent, and temperature, however, lower the barriers toward dispersion and can be exploited to achieve better initial orientations. This was the case for DMF relative to DMAc and DMSO in the absence of polymers. The presence of PMMA had a positive effect in all solvents due to binding affinity to SWCNTs, best in DMSO.

For CNT-PAN composites, after solvent removal, we analyzed for the first time the relationship between initial PAN crystallinity and the computed shear stability of the composites down to the molecular scale. Intermediate crystallinity of 50%, or higher, improved the shear strength by 20-30%, and showed that SWCNTs fared better than MWCNTs. The absolute numbers for the shear strength (10-20 MPa) are also closely in the range expected in experiments, showing that the simulation techniques can now yield quantitative data.

A key parameter for composite properties, before carbonization into carbon nanofiber, was identified to be the interfacial area between CNTs and the polymer per composite unit volume or composite unit mass. Higher interfacial area per unit volume lead to an increased glass transition temperature and better interfacial alignment of the polymer chains. The specific interfacial area is easy to control in modeling and simulation while in experiment it depends on the degree of bundling of CNTs and precise knowledge of the prevailing CNT diameters. Higher levels of control and rational design of nanocomposite and nanofiber properties in experiment can therefore be linked to measuring and controlling CNT diameters and bundle size. Ideally, small CNT diameter and full dispersion leads to higher Tgs and interfacial shear strength, however, in some

cases larger diameter with smaller bundle size can be more effective than small diameter with large bundle size. Another promising route for property improvements is interphase engineering such as PMMA wrapping onto CNTs as identified by Kumar. Nanotube diameters in the range 0.8 to 1.1 nm lead to better PMMA binding and interphase stabilization than larger diameters.

Going forward, this work shows that simulation can be helpful in determining which CNT characteristics and interphase morphologies improve dispersion, alignment, and mechanical properties, and the methods are applicable to other carbon-materials and low-density materials in general. Key to the effectiveness of simulations is iterative feedback between simulation and the experiment alongside with reliable potentials, the use of the same measures for crystallinity and characterization as in experiment, and clear deliverables to be able to compare with laboratory measurements.

SECTION II – Publications and Theses

Publications during the course of this grant:

1. A. T. Chien, S. Cho, Y. Joshi, S. Kumar, "Electrical Conductivity and Joule Heating of Polyacrylonitrile/Carbon Nanotube Composite Fibers", *Polymer*, **55**, p. 6896 – 6905 (2014). DOI: 10.1016/j.polymer.2014.10.064
2. A. T. Chien, H. C. Liu, B. A. Newcomb, C. Xiang, J. M. Tour, S. Kumar, "PAN fibers containing graphene oxide nanoribbons", *ACS Applied Materials and Interfaces*, **7**, 5281 - 5288 (2015). DOI:10.1021/am508594p
3. Y. Liu, H. G. Chae, Y. H. Choi, S. Kumar, "Preparation of low density hollow carbon fibers by bi-component gel spinning method", *J. Mater Sci.*,**50**, 3614 - 3621 (2015). DOI: 10.1007/s10853-015-8922-3
4. X. Yan, H. Dong, Y. Liu, B. A. Newcomb, H. G. Chae, S. Kumar, Z. Xiao, T. Liu, "Effect of processing conditions on the dispersion of carbon nanotubes in polyacrylonitrile solutions", *J. Appl. Polym. Sci.*, **132** (26)**,** article number 42177 (2015). DOI: 10.1002/APP.42177
5. R. Vijay, M. Gupta, H. G. Chae, T. Liu, S. Kumar, "Investigation of Polyacrylonitrile Solution Inhomogeneity by Dynamic Light Scattering". *Polymer Engr and Sci.,* (2015). DOI: 10.1002/pen.24084
6. B. A. Newcomb, L. A. Giannuzzi, K. M. Lyons, P. V. Gulgunje, K. Gupta, Y. Liu, M. G. Kamath, K. McDonald, J. Moon, B. Feng, G. P. Peterson, H. G. Chae, S. Kumar, "High resolution transmission electron microscopy study on polyacrylonitrile/carbon nanotube based carbon fibers and the effect of structure development on the thermal and electrical conductivities", *Carbon*, **93**, 502-514 (2015). http://dx.doi.org/10.1016/j.carbon.2015.05.037
7. X. Yan, H. Dong, Z. Xiao, T. Liu, H. G. Chae, S. Kumar, "Effect of high-shear mixing by twin-screw extruder on the dispersion and homogeneity of polyacrylonitrile/carbon nanotube composite solution", *Polymer Composites*, (2015). DOI:10.1002/pc.23631
8. H. G. Chae, B. A. Newcomb, P. V. Gulgunje, Y. Liu, K. Gupta, M. G. Kamath, K. M. Lyons, S. Ghoshal, C. Pramanik, L. A. Giannuzzi, K. Sahin, I. Chasiotis, S. Kumar, "High strength and high modulus carbon fibers", *Carbon*, **93**, 81-87 (2015). http://dx.doi.org/10.1016/j.carbon.2015.05.016

9. H. Chang, A. T. Chien, H. C. Liu, P. H. Wang, B. A. Newcomb, and S. Kumar, "Gel Spinning of Polyacrylonitrile/Cellulose Nanocrystal Composite Fibers", *ACS Biomaterials Science and Engineering*, (2015). http://dx.doi.org/10.1021/acsbiomaterials.5b00161
10. A. A. B. Davijani and S. Kumar, "Ordered wrapping of poly (methyl methacrylate) on single wall carbon nanotubes, *Polymer*,**70**, 278-281 (2015). http://dx.doi.org/10.1016/j.polymer.2015.06.018
11. B. A. Newcomb, P. V. Gulgunje, K. Gupta, M. G. Kamath, Y. Liu, L. A. Giannuzzi, H. G. Chae, S. Kumar, "Processing, structure, and properties of gel spun PAN and PAN/CNT fibers and gel spun PAN based carbon fibers", *Polymer Engineering and Science*, 2015. DOI 10.1002/pen.24153
12. P. V. Gulgunje, B. A. Newcomb, K. Gupta, H. G. Chae, T. Tsotsis, S. Kumar, "Low density and high-modulus carbon fibers from polyacrylonitrile with honeycomb structure", *Carbon*,**95**, 710-714 *(2015).* DOI: 10.1016/j.carbon.2015.08.097
13. H. Clive Liu, A. T. Chien, B. A. Newcomb, Y. Liu, S. Kumar, "Processing, structure and properties of lignin and CNT incorporated PAN based carbon fibers", *ACS Sustainable Chemistry and Engineering*, (2015). http://dx.doi.org/10.1021/acssuschemeng.5b00562
14. B. A. Newcomb, P. V. Gulgunje, Y. Liu, K. Gupta, M. G. Kamath, C. Pramanik, S. Ghoshal, H. G. Chae, S. Kumar, "Polyacrylonitrile solution homogeneity study by dynamic shear rheology and the effect on the carbon fiber tensile strength", *Polymer Science and Engineering*, (2015). DOI 10.1002/pen.24261
15. H. C. Liu, A.T. Chien, B. A. Newcomb, A. A. B. Davijani, S. Kumar, "Stabilization Kinetics of Gel Spun Polyacrylonitrile/Lignin Blend fiber", *Carbon* **101,** 382 - 389 (2016). http://dx.doi.org/10.1016/j.carbon.2016.01.096
16. H. Chang, J. Luo, A. Davijani, A.T. Chien, P. H. Wang, H. Liu, S. Kumar, "Individually dispersed wood based cellulose nano crystals", *ACS Applied Materials and Interfaces*, **8**, 5768 – 5771 (2016). http://dx.doi.org/10.1021/acsami.6b00094
17. A. A. B. Davijani, H. C. Liu, K. Gupta, S. Kumar, "High surface area electrodes derived from polymer wrapped carbon nanotubes for enhanced energy storage devices", *ACS Applied Materials and Interfaces*, 8, 24918 – 24923 (2016). DOI:10.1021/acsami.6b08845
18. H. Heinz, "Adsorption of Biomolecules and Polymers on Silicates, Glasses, and Oxides: Mechanisms, Predictions, and Opportunities by Molecular Simulation", *Curr. Opin. Chem. Eng.* **11**, 34-41 (2016). DOI: 10.1016/j.coche.2015.12.003
19. H. Heinz, H. Ramezani-Dakhel, "Simulations of Inorganic–Bioorganic Interfaces to Discover New Materials: Insights, Comparisons to Experiment, Challenges, and Opportunities", *Chem. Soc. Rev.* **45**, 412-448 (2016). DOI: 10.1039/C5CS00890E
20. K. Gupta, T. Liu, R. Kavian, H. G. Chae, G. H. Ryu, Z. Lee, S. W. Lee, S. Kumar, "High surface area carbon from polyacrylonitrile for high performance electrochemical capacitive energy storage", *Journal of Materials Chemistry A*, **4,** 18294 - 18299 (2016), DOI: 10.1039/C6TA08868F
21. H. Chang, J. Luo, H. C. Liu, A. A. B. Davijani, P. H. Wang, S. Kumar, "Orientation and interfacial stress transfer of cellulose nanocrystal nanocomposite fibers", *Polymer*, **110**, 228-234 (2017). http://dx.doi.org/10.1016/j.polymer.2017.01.015

22. H. C. Liu, C. C. Tuan, A. A. B. Davijani, P. H. Wang, H. Chang, C. P. Wong, S. Kumar, "Rheological behavior of polyacrylonitrile and polyacrylonitrile/lignin blends", *Polymer*, **111**, 177 - 182 (2017). http://dx.doi.org/10.1016/j.polymer.2017.01.043
23. H. Chang, J. Luo, P. V. Gulgunje, S. Kumar, "Structural and Functional Fibers", *Annual Review of Materials Research*, **47,** 331-359 (2017). Doi: 10.1146/annurev-matsci-120116-114326
24. J. Luo, H. Chang, A.A.B. Davijani, H.C. Liu, P. H. Wang, R. J. Moon, S. Kumar, "Influence of high loading of cellulose nanocrystals in polyacrylonitrile composite films", *Cellulose*, **24**, 1745 - 1758 (2017). DOI: http://link.springer.com/article/10.1007/s10570-017-1219-8
25. B. A. Newcomb, H. G. Chae, L. Thomson, J. Luo, J. B. Baek, S. Kumar, "Reinforcement efficiency of carbon nanotubes and their effect on crystal-crystal slip in poly(ether ketone)/carbon nanotube composite fibers", *Composite Science and Technology*, **147,** 116 - 125 (2017) . DOI: 10.1016/j.compscitech.2017.05.011
26. H. Chang, J. Luo, H. C. Liu, A. Davijani, P. H. Wang, G. S. Lolov, R. M. Dwyer, S. Kumar, "Ductile polyacrylonitrile fibers with high cellulose nanocrystals loading", *Polymer*, **122**, 332-339 (2017). http://dx.doi.org/10.1016/j.polymer.2017.06.072
27. A. A. B. Davijani, H. Chang, H. C. Liu, J. Luo, S. Kumar, "Stress transfer in nano composites enabled by poly(methyl methacrylate) wrapping of carbon nanotubes", *Polymer*, **130,** 191-198 (2017). https://doi.org/10.1016/j.polymer.2017.10.002
28. C. Pramanik, J. R. Gissinger, S. Kumar, H. Heinz, Carbon Nanotube Dispersion in Solvents and Polymer Solutions: Mechanisms, Assembly, and Preferences, *ACS Nano*, 11, 12805 - 12816 (2017). DOI: 10.1021/acsnano.7b07684
29. J. Luo, N. Semenikhin, H. Chang, R. J. Moon, S. Kumar, "Post-sulfonation of cellulose nanofibrils with a one-step reaction to improve dispersibility", Carbohydrate Polymers, 181, 247-255 (2018). https://doi.org/10.1016/j.carbpol.2017.10.077
30. J. R. Gissinger, C. Pramanik, B. Newcomb, S. Kumar, H. Heinz, "Nanoscale Structure-Property Relationships of Polyacrylonitrile/CNT Composites as a Function of Polymer Crystallinity and CNT Diameter", ACS Applied Materials and Interfaces, 10, 1017 – 1027 (2018). DOI:10.1021/acsami.7b09739
31. C. Pramanik, D. Nepal, M. Nathanson, J. R. Gissinger, A. Garley, R. J. Berry, A. Davijani, S. Kumar, H. Heinz, "Molecular Engineering of Interphases in Polymer/Carbon Nanotube Composites to Reach the Limits of Mechanical Performance", Composites Science and Technology, (2018). DOI: 10.1016/j.compscitech.2018.04.013
32. R. Vijay, P. Gulgunje, K. Gupta, M. G. Kamath, Y. Liu, C. Pramanik, B. Newcomb, H. G. Chae, S. Kumar, "Correlation between inhomogeneity in polyacrylonitrile spinning dopes and carbon fiber tensile strength", Polymer Engineering and Science, (2018). DOI: 10.1002/pen.24947

A number of additional manuscripts are currently being prepared for publication.

Ph.D. thesis on carbon fiber related topics completed during the course of this project (2014-2018)

An-Ting Chien, "Multi-functional PAN-based Composite Fibers", Ph.D. Thesis, Georgia Tech, 2014.

Bradley Allen Newcomb, “Gel Spun PAN and PAN/CNT Based Carbon Fibers: From Viscoelastic Solution to Elastic Fiber”, Ph.D. Thesis, Georgia Tech, 2015.

Amir Ahmad Bakhtiary Davijani, “Effect of poly (methyl methacrylate) wrapping on the structure and properties of CNT films and polymer/CNT films and fiber”, Ph.D. Thesis, Georgia Tech, 2016.

Hsiang-Hao Clive Liu, “Gel spun polyacrylonitrile based carbon fibers containing lignin and carbon nanotubes”, Ph.D. Thesis, Georgia Tech, 2017.

Huibin Chang, “Studies on polyacrylonitrile/cellulose nanocrystals composite precursor and carbon fibers”, Ph.D. Thesis, Georgia Tech, 2017

Jeffrey Luo, “Processing, structure, and properties of polyacrylonitrile films and fibers with high nanocellulose loading”, Ph.D. Thesis, Georgia Tech, 2018

A number of additional studies towards Ph.D. theses are currently ongoing. The work on lignin and cellulose was also supported by graduate fellowships from The Renewable Bioproducts Institute at Georgia Tech.

SECTION III – Unpublished Studies

Unpublished and on-going modeling studies:

Modeling work in preparation for publication includes an analysis of the interaction of long-chain PAN with CNTs in different solvents and as a function of temperature, as well as a comprehensive analysis of PMMA wrapping onto CNTs of different diameters at different temperatures. A third work in progress is the final and comprehensive parameterization of graphitic materials including virtual π electrons, which will be compatible with various energy expressions and is co-sponsored by a current NASA grant.

The analysis of PAN/CNT interaction in various solvents is particularly relevant for increased molecular weight that is closer to experimental conditions than prior all-atom modeling studies. We represented such longer PAN chains in the molecular dynamics simulations by a chain length of 100-mers. Equilibration and sampling of conformations required from multiple replicas and annealing prior to reaching convergence over 50 ns simulation time at the chosen target temperatures of 25 ºC and 75 ºC. These temperatures are, among others, used in the laboratory preparation of carbon fiber precursors. Representative polymer conformations at 10 wt% concentration indicate no strong or prolonged binding, however, spontaneous contacts of a number of monomers with the CNT surface are seen (Figure 1). This general trend is the same at both temperatures (Figure 1a-f). Surface contacts between PAN and CNTs involve hydrogen atoms, carbon atoms, and nitrogen atoms whereby nitrile groups often align with the direction of C-C bonds and orient themselves parallel to the CNT surface (Figure 1 g-i). This orientation is, in principle, favorable for carbonization reactions to form graphitic overlayers, however, the orientation preference occurs only with a certain probability. Differences between the solvents and

temperatures have been mapped out more quantitatively by using the time-average distance of individual polymer chains from the surface and the number of monomers in close contact with the surface (Figure 2). The results show a distribution of distances that is closer to the surface at 25 ºC (Figure 2a) compared to 75 ºC (Figure 2c). At the same time, the solvent has a visible effect. DMAc, for example, allows better binding of PAN to CNTs at lower temperature, however, the other solvents DMF and DMSO allow better binding at higher temperature. The same trend is also seen for the number of close contacts of monomers with the CNT surface (Figures 2b, d). Another measure to characterize polymer dynamics is the radius of gyration R_g, which equals about 70 Å for a fully extended PAN-100 chain. The radius of gyration found in the precursor solutions is between 15 and 40 Å (Figure 3), thus clearly corresponding to more coiled and folded conformations (as seen in Figure 1). At low concentration of PAN in solution of 1 wt%, the radius of gyration in DMF was independent of temperature, perhaps with a small decrease at higher temperature in the presence of CNTs related to poor CNT binding (Figure 3a). In DMAc and DMSO, R_g increased significantly for higher temperature when no CNTs were present and only slightly or not at all when CNTs were present. Overall, it appears that CNTs mitigate effect of temperature on the radius of gyration. At higher concentration of PAN in solution of 10 wt%, the radius of gyration is almost the same regardless of the temperature and of the solvent (Figure 3b). More significant interactions between the polymer chains introduce steric effects and lead to an intermediate value of R_g of ~25 Å. The trend of slightly increasing radius of gyration at higher temperature in DMAc and DMSO in the absence of CNTs persists but is much weaker compared to 1 wt% concentration.

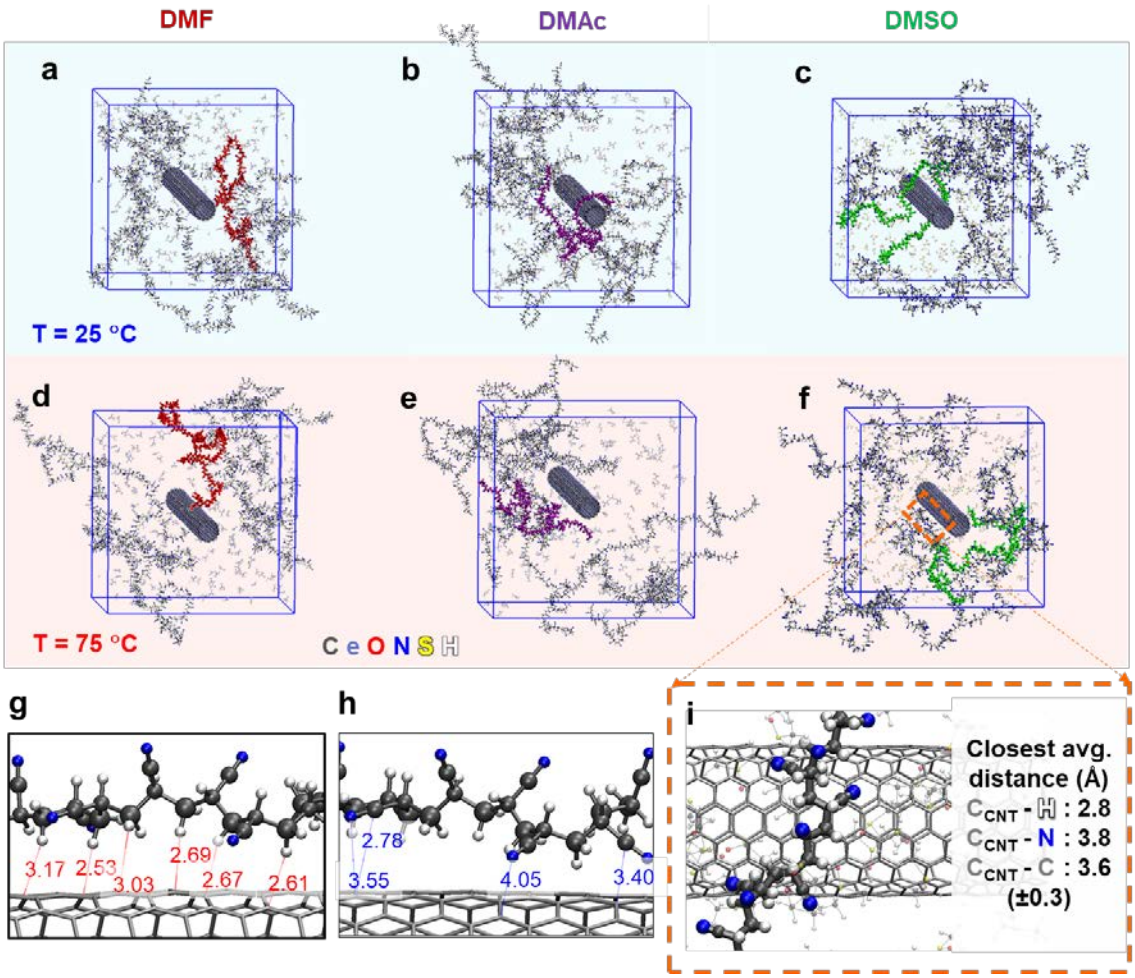

Figure 1. Interaction of PAN_{100} chains with a CNT in concentrated solution (10 wt%) as a function of solvent and temperature in equilibrium. (a-c) 3D distribution of PAN chains surrounding a CNT in DMF, in DMAc, and in DMSO at 298K. The statistically closest chain interacting with CNT surface is highlighted in color. (d-f) PAN polymer distribution in DMF, in DMAc, and in DMSO at 348 K. The statistically closest chains to the CNT are also highlighted in color. (g, h) Magnified representation of interactions between a segment of the polymer chain with the CNT surface. Typical distances between carbon atoms on the CNT surface and functional groups in interacting PAN segments are indicated. Solvent molecules and π-electrons of the CNT are not shown for clarity in this view. (i) A frequently observed molecular orientation of PAN interacting with CNT surface in DMSO is transverse with respect to the CNT axis (inset from f). A parallel orientation of C≡N groups to the CNT surface can be seen and hydrogen atoms are sometimes oriented perpendicular to the CNT surface. Closest average distances between atoms in the polymer and the CNT surface atoms are listed.

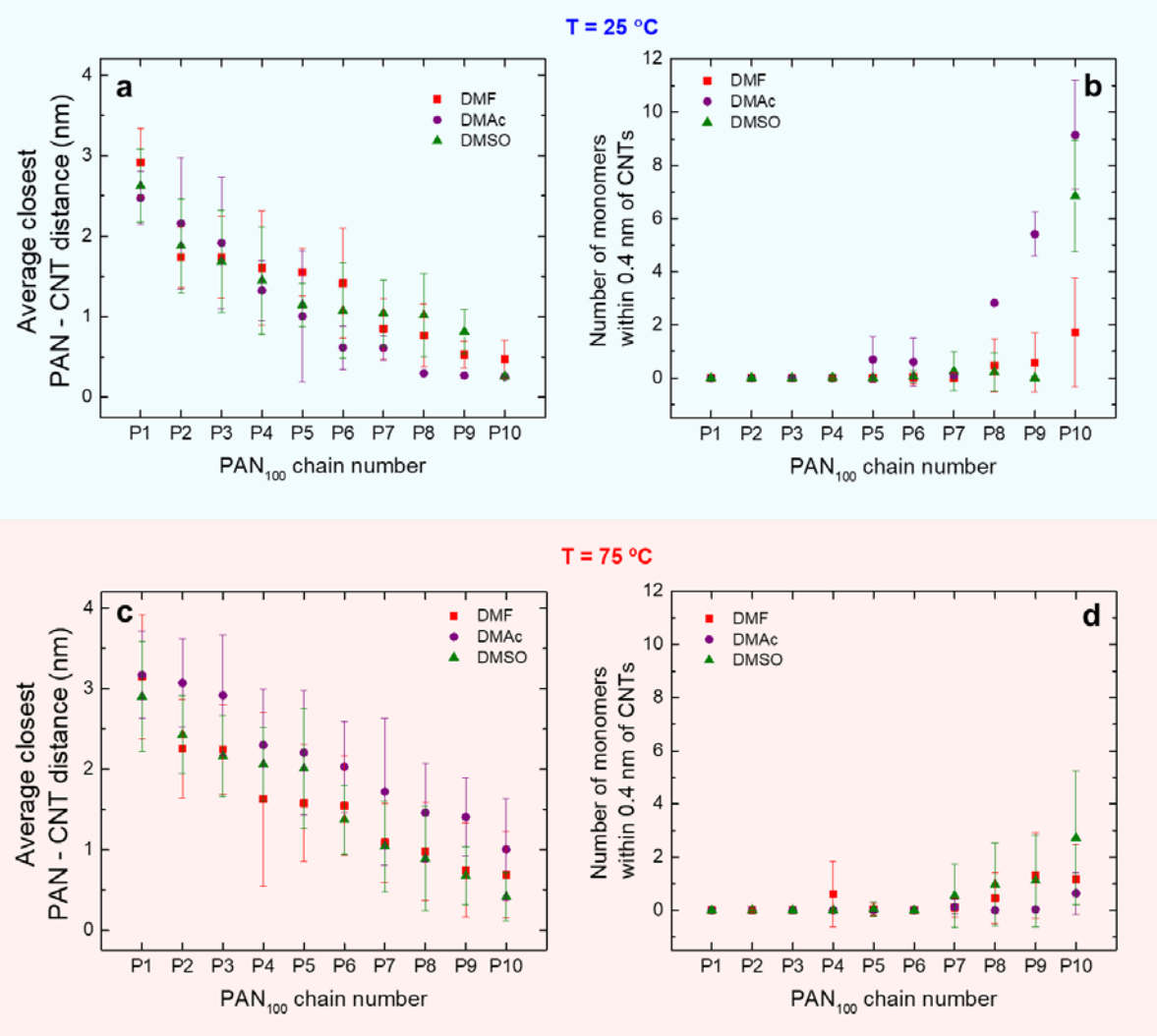

Figure 2. Distance of ten PAN_{100} polymers from the CNT surface as a function of solvent and temperature at a concentration of 10 wt%. The average closest distance and the number of acrylonitrile monomers within 4 Å distance are shown. (a) Average closest PAN-CNT distance at 25 ºC. (b) Number of PAN monomers within 4 Å distance from the CNT surface at 25 ºC. (c) Average closest PAN-CNT distance at 75 ºC. (d) Number of PAN monomers within 4 Å distance from the CNT surface at 75 ºC. Only few out of 10 polymers are in close contact with the CNT for an extended period of time. Higher temperature increases the average minimum distance and reduces polymer binding. PAN binding increases in the order DMF ~ DMSO < DMAc at 25 ºC and changes to the order DMAc < DMF < DMSO at 75 ºC.

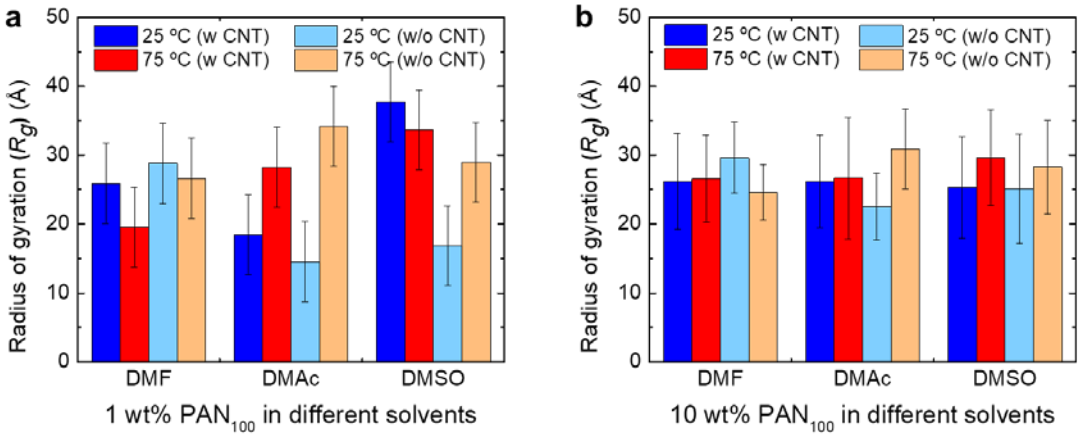

Figure 3. Radius of gyration of PAN_{100} for low (1 wt%) and high (10 wt%) concentrations in solvents as a function of temperature, with and without CNT. (a) Dilute solution with 1 wt%. (b) Concentrated solution with 10 wt%. PAN in DMF tends to contract slightly at higher temperature and CNTs do not significantly affect conformations due to lack of binding at both temperatures. PAN in DMAc expands at higher temperature and the presence of CNTs slightly diminishes this effect sterically (negligible binding at lower temperature). PAN in DMSO expands at higher temperature in the absence of CNTs. PAN binds to CNTs in DMSO and significantly stretches in the presence of CNTs at low concentration. At higher concentration, steric effects limit stretching in the presence of CNTs. The corresponding fully extended PAN_{100} chain would be about 210 to 250 Å long with a R_g of 60 to 72 Å ($R_g^2 = L^2/12$ for a rod).

Efforts for the analysis of PMMA wrapping onto CNTs thus far have revealed an energy penalty for extended conformations relative to coiled/semi-wrapped and wrapped conformations for a range of CNT diameters from 0.8 to 2.0 nm and temperatures from -50 ºC to +100 ºC (Figure 4). These data are in agreement with experimental observations that are available for some of the cases (Polymer 2015, 70, 278-281). Orderly wrapped conformations show a global energy minimum from 0.8 to 1.0 nm diameter and again at >1.5 nm diameter of CNTs, then corresponding to a preference for ordered or disordered wrapping (Figure 4c versus Figure 4d). The data and trends also show only a limited dependence on temperature in the range from -50 ºC to +100 ºC. For CNTs of 2 nm size, ordered wrapping was preferred at a temperature of 75-100 ºC. Pending some refinements and comparisons to measurements, these results will be published separately and can be helpful to optimize the stability of CNT dispersions in the laboratory.

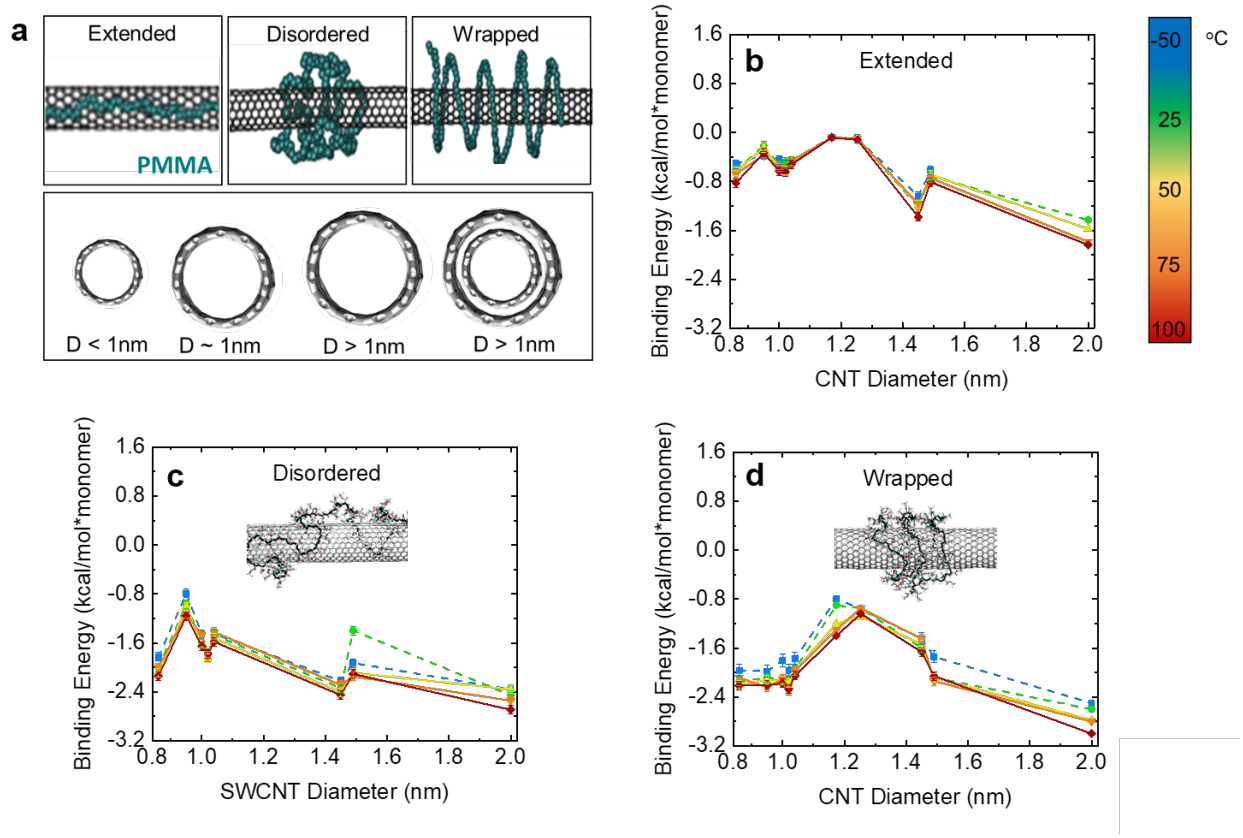

Figure 4. Stability of PMMA interphases on CNTs as a function of CNT type and temperature. (a) Different states of polymer-CNT interaction and types of CNTs investigated. (b) PMMA binding energies to various CNTs in extended conformations are negative (= favorable). (c) Disordered semi-wrapped conformations are more favorable in all cases. (d) Ordered wrapped conformations are similarly stable as the disordered/semi-wrapped conformations. Highest stability is seen for 0.8 to 1.05 nm CNTs, less stability relative to disordered wrapped for 1.05 to 1.5 nm CNTs, and about equal stability between 1.5 nm and 2.0 nm. The influence of temperature is not very strong overall, however, wrapped PMMA conformations are preferred for 2 nm CNTs at higher temperature.

Another effort is the broader implementation of the new atomistic force field parameters for graphitic materials with virtual π electrons. The first generation parameters are published and available on the website of the Interface Force Field to which the parameters have been added (http://bionanostructures.com/interface-md). The full-scale validation and integration into multiple force fields for broad applicability in materials and biological/biomaterials system simulations (CHARMM, AMBER, OPLS-AA) is still in progress and will be published in a separate model-focused paper. Several groups are already using the new force field as the accuracy of computed interfacial and mechanical properties is about 10 times higher relative to prior models, which have deviations up to 100%.

PAN/BNNT Fibers

[With contributions from Huibin Chang, Mingxuan Lu , Jeffrey Luo, Pedro J. Arias Monje, Jin Gyu Park (FSU), Richard Liang (FSU) , Cheol Park (NASA – Langley) and Satish Kumar]

Polyacrylonitrile (PAN)/boron nitride nanotube (BNNT) composite fibers were spun using gel spinning method and the resulting carbon fibers were processed after the fibers were stabilized in air and subsequently carbonized in nitrogen. Both stabilization and carbonization were done in batch process. PAN fibers containing 1 wt% BNNTs show comparable drawability to the control PAN fiber while the drawability of composite fibers significantly decreases as BNNT concentration increased to 5 wt%. Differential scanning calorimetry suggests that the presence of BNNTs reduces the activation energy of oxidation and crosslinking reactions but has little effect on the activation energy of cyclization reaction. In the PAN/BNNT based carbon fibers, the graphitic carbon structure that formed in the vicinity of BNNT at 1300°C carbonization temperature was directly observed by transmission electron microscopy. Orientation and interfacial stress transfer in PAN/BNNT fibers were determined by Raman spectroscopy.

The mechanical properties of PAN and PAN/BNNT composite fiber at their maximum draw ratio are listed in Table 1. Compared to the control PAN fiber, PAN/BNNT composite fiber containing 1wt% BNNTs shows similar maximum draw ratio. For the mechanical properties, PAN/BNNT-1 composite fiber show slightly lower average values of tensile strength and modulus than those of PAN fibers. Both PAN and PAN/BNNT-1 fibers show similar elongation at break and work of rupture. However, when BNNTs concentration increases from 1 to 5 wt%, the maximum draw ratio of fibers significantly decreased from 22x to 12x. However, PAN/BNNT-1 and PAN/BNNT-5 composite fibers show comparable tensile strength and tensile modulus. This suggests that BNNTs could potentially be used as nano filler to reinforce the polymer materials. **However, based on PAN/CNC studies, it may be possible to further increase BNNT concentration, as well as elongation to break after suitable functionalization of BNNT.** We also note that the BNNTs used in this study had 50% impurity. When high purity BNNT are used, then higher mechanical properties fibers can be expected.

The structural parameters of the fibers at their maximum draw ratio are listed in Table 2. At similar maximum draw ratio, both PAN and PAN/BNNT-1 fibers show similar PAN crystallinity. The PAN chain orientation is slightly lower in PAN/BNNT-1 composite fiber than in the control PAN fiber. However, PAN/BNNT-1 fiber show higher PAN crystal size of 11.9 nm, which is about 27% larger than 9.4 nm PAN crystal size in the control PAN fiber. **This shows that the presence of small amount of BNNT in the PAN matrix can promote the PAN crystal growth during the drawing process.** As the BNNTs concentration increased from 1 to 5 wt%, the maximum draw ratio significantly decreased. This leads to the less oriented PAN chain and smaller PAN crystal size in the PAN/BNNT-5 composite fibers as compared to PAN/BNNT-1 fiber. As compared to the control PAN fiber, PAN/BNNT-5 composite fiber shows similar PAN crystallinity (58%) and larger PAN crystal size (10.6 nm for PAN/BNNT-5 vs 9.4 nm for PAN fiber).

Table 1. Mechanical properties of PAN and PAN/BNNT composite precursor fibers.

	PAN	PAN/BNNT-1	PAN/BNNT-5
Total maximum draw ratio	20	22	12
Linear density (dtex)	1.4 ± 0.1	1.0 ± 0.1	1.9 ± 0.5
Theoretical density (g/cm^3)	1.18	1.19	1.23
Effective diameter (μm)	12.4 ± 0.6	10.4 ± 0.7	13.9 ± 1.9
Tensile modulus (GPa)	18.5 ± 1.1	17.3 ± 0.6	17.7 ± 1.2
Tensile strength (MPa)	902 ± 60	826 ± 72	789 ± 96
Elongation at break (% strain)	8.0 ± 1.0	8.0 ± 0.7	8.8 ± 0.9
Work of rupture (MPa)	35.4 ± 3.2	33.7 ± 5.3	36.6 ± 2.4

Table 2. Structural parameters of PAN and PAN/BNNT composite precursor fibers

	PAN fiber	PAN/BNNT-1	PAN/BNNT-5
Total maximum draw ratio	20	22	12
PAN crystallinity (%)	58	59	58
PAN crystal size (nm)	9.4	11.9	10.6
f_{pan}	0.85	0.83	0.70
f_{BNNT}	-	-	0.61
$PAN_{2\theta meridional}$	39.2	39.0	39.4

Mechanical properties of carbonized fibers are summarized in Table 3. When stabilized and carbonized in batch process, tensile strength and tensile modulus of PAN based carbon fiber are 1.7 GPa and 273 GPa, respectively. Tensile strength and tensile modulus of the PAN/BNNT-1 based carbon fiber are 2.0 and 258 GPa, respectively. Even though PAN/BNNT-5 fibers show a much lower total draw ratio of 12x, PAN/BNNT-5 based carbon fibers exhibit tensile strength of 1.5 GPa and a tensile modulus of 243 GPa. Various structural parameters of various carbonized fibers are listed in Table 4. A comparison among PAN and PAN/BNNT based carbon fibers suggests the presence of BNNT affects the carbon structure as compared to the PAN based carbon fiber structure. Regardless of the precursor fiber draw ratio, PAN/BNNT based carbon fibers show increased crystal size of (002) and (10) planes.

Table 3. Mechanical properties of carbonized PAN and PAN/BNNT composite fibers

	PAN fiber	PAN/BNNT-1 fiber	PAN/BNNT-5 fiber
Total draw ratio	20	22	12
Linear density (dtex)	0.8 ± 0.1	0.5 ± 0.1	0.8 ± 0.1
Theoretical density (g/cm^3)	1.8	1.8	1.8
Effective diameter (μm)	7.7 ± 0.2	6.0 ± 0.4	7.6 ± 0.5
Tensile modulus (GPa)	273 ± 5	258 ± 9	243 ± 3
Tensile strength (GPa)	1.7 ± 0.3	2.0 ± 0.2	1.5 ± 0.4
Elongation at break (% strain)	0.6 ± 0.2	0.9 ± 0.3	0.6 ± 0.2

High resolution TEM images of PAN/BNNT based carbon fibers are shown in Figure 5. In carbonized PAN, away from the BNNT, turbostratic crystallites are observed. However, a highly ordered graphitic region is observed surrounding the BNNT. **In these carbon fibers, up to 10 graphitic layers are developed beyond the BNNT, which clearly shows the formation and growth of the BNNT templated graphitic structure.** The graphitic formation around CNT in PAN/CNT based carbon fibers has been reported previously. This templating phenomenon in BNNT or CNT based carbon fibers is attributed to the fact that BNNT is structurally analogues of CNT.

If higher BNNT concentration can be used in PAN, then it should be possible to further increase the thermal conductivity of the carbon fiber, while also enhancing its neutron absorption cross-section. Following PAN/CNC study, this may be possible using BNNT functionalization.

Table 4. Structural parameters of carbonized PAN and PAN/BNNT fibers at 1300°C

	PAN	PAN/BNNT-1	PAN/BNNT-5
Total draw ratio	20	22	12
$d_{(002)}$ [a] (nm)	0.349	0.349	0.346
$L_{(002)}$ [b] (nm)	1.43	1.44	1.87
$L_{(10)}$ [c] (nm)	2.23	2.42	2.50
f_{002} [d]	0.80	0.81	0.82
Z_{002} [e] (deg)	28.7	27.9	27.8

[a] $d_{(002)}$: d-spacing of (002) plane at $2\theta \sim 26°$.
[b] Crystal size of (002) plane at $2\theta \sim 26°$, according to Scherrer's equation with $K = 0.9$
[c] Crystal size of (10) plane at $2\theta \sim 43°$, according to Scherrer's equation with $K = 0.9$
[d] orientation factor of (002) plane
[e] Full-width at half-maximum (FWHM) from azimuthal scans of (002) plane at $2\theta \sim 26°$.

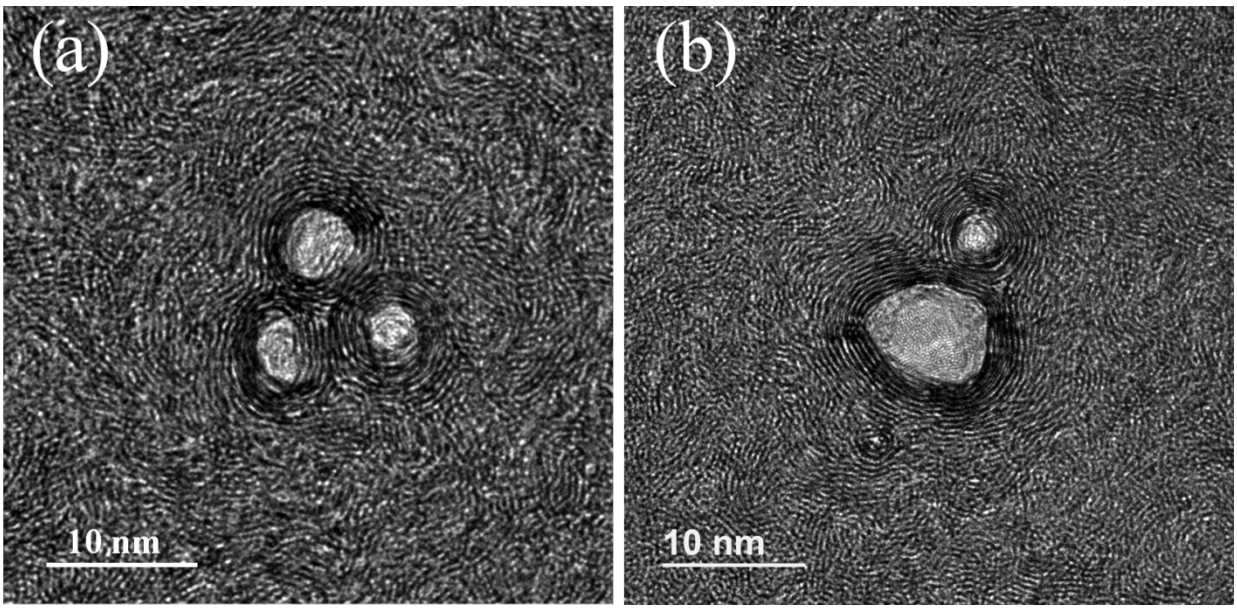

Figure 5. High resolution transmission electron micrographs of fiber cross-sectional images of PAN/BNNT based carbon fibers. (a) PAN/BNNT-1 and (b) PAN/BNNT-5. Both TEM images provide direct evidence of graphitic templating and epitaxial growth on the outer most surface of BNNT, and no de-bonding between carbonized PAN and BNNT.

PAN/CNC Fibers

(With contributions from Huibin Chang, Jeffrey Luo, H. Clive Liu, Songlin Zhang (FSU), Jin Gyu Park (FSU), Richard Liang (FSU), and Satish Kumar)

Polyacrylonitrile (PAN) fibers containing up to 40 wt% cellulose nanocrystals (CNC) have been successfully stabilized and carbonized to make carbon fibers. Under the batch process, PAN/CNC based carbon fibers exhibit a tensile strength in the range of 1.8 – 2.3 GPa, and tensile modulus in the range of 220 - 265 GPa, which are comparable to the control PAN-based carbon fibers. Based on the transmission electron microscopy study, individually distributed CNC regions surrounded by PAN matrix were observed in the stabilized and carbonized fibers. Carbonized fibers show clear boundaries between PAN and CNCs based carbon regions. This study shows that biphasic carbon fibers can be made from the PAN/CNC system.

Mechanical properties of carbonized fibers (PAN and PAN/CNC-40) at 1000, 1100 and 1200 °C are listed in Table 5. The mechanical properties of carbonized fibers at 1300 and 1400 °C are listed in Table 6. As carbonization temperature increases to 1400°C, as compared to fibers carbonized at lower temperature, PAN based carbon fibers and PAN/CNC-40 based carbon fibers show similar tensile strength, which is about 1.9 GPa. To study the effect of CNCs concentration on the carbon fiber properties, PAN/CNC-10 and PAN/CNC-20 fibers are also carbonized at 1300 and 1400°C. At 1400°C carbonization temperature, both PAN/CNC-10 and PAN/CNC-20 based carbon fibers show slightly higher average tensile strength (2.3 GPa) than PAN based carbon fiber (1.6 GPa), and they show comparable tensile modulus (265 GPa for PAN/CNC-10 based carbon fiber, and 252 GPa for PAN/CNC-20 based carbon fiber) as compared to PAN based carbon fiber (257 GPa). Higher properties will be achieved when stabilization and carbonization is carried out on multi-zone continuous line.

Table 5. Tensile properties of PAN and PAN/CNC-40 based carbon fibers.

	PAN*			PAN/CNC-40*		
Carbonization Temperature	1000 °C	1100 °C	1200 °C	1000 °C	1100 °C	1200 °C
Diameter (μm)	8.2 ± 0.7	7.6 ± 0.5	8.1 ± 0.4	7.0 ± 0.3	6.9 ± 0.2	7.0 ± 0.3
Modulus (GPa)	203 ± 16	220 ± 5	226 ± 8	189 ± 12	190 ± 5	205 ± 4
Strength (GPa)	1.9 ± 0.5	2.0 ± 0.4	2.2 ± 0.3	1.7 ± 0.2	1.8 ± 0.2	1.7 ± 0.2
Elongation at break (%)	0.7 ± 0.2	0.6 ± 0.1	1.0 ± 0.1	0.9 ± 0.1	1.0 ± 0.1	0.7 ± 0.1

* Precursor fiber at a draw ratio of 23.

Table 6. Tensile properties of various carbon fibers.

	PAN*		PAN/CNC-10*		PAN/CNC-20*		PAN/CNC-40*	
Carbonization Temperature	1300 °C	1400 °C	1300 °C	1400 °C	1300 °C	1400 °C	1300 °C	1400 °C
Diameter (μm)	7.7±0.4	8.1 ± 0.3	7.4 ± 0.4	7.5 ± 0.3	6.2 ± 0.1	6.0 ± 0.4	7.3 ± 0.3	7.1 ± 0.3
Modulus (GPa)	251 ± 27	257 ± 8	251 ± 10	265 ± 11	246 ± 12	252 ± 9	226 ± 18	220 ± 7
Strength (GPa)	1.9 ± 0.4	1.6 ± 0.4	1.8 ± 0.3	2.3 ± 0.4	2.3 ± 0.5	2.3 ± 0.5	1.8 ± 0.4	1.9 ± 0.4
elongation at break (%)	0.7 ± 0.1	0.6 ± 0.1	0.7 ± 0.1	0.8 ± 0.1	0.9 ± 0.2	0.9 ± 0.2	0.7 ± 0.1	0.9 ± 0.2

* Precursor fiber at a draw ratio of 23.

To study the effect of CNCs on the structure of PAN based carbon fibers, carbonized fibers were characterized by Raman spectroscopy. The Raman spectra of carbon fibers exhibits a disorder band (D-band at ~ 1350 cm^{-1}) and graphitic band (G-band at ~ 1580 cm^{-1}). The ordered crystalline carbon percent in the carbon materials could be estimated from the I_D/I_G peak intensity ratio. The lower the I_D/I_G value, the more ordered is carbon in the carbon fibers. The Raman spectra of fibers carbonized at 1300 °C are shown in Figure 6. I_D/I_G values of all composite based carbon fibers show relatively low values (from 2.1 to 2.3) than that of PAN based carbon fibers (2.5). The reasons of more ordered crystalline carbon in PAN/CNC based carbon fibers were investigated by high resolution TEM, which relates to the high crystalline CNC and potentially highly ordered carbon around the boundaries between PAN and CNC based carbon regions.

Integrated WAXD scans of precursor, stabilized, and carbon fibers are shown in Figure 7. Carbonized fibers show two distinct peaks at $2\theta \approx 26°$, and ~43°, which are (002) and (100) (101) planes of carbon structure, respectively. Structural parameters of various carbon fibers are listed in Table 7. For PAN and PAN/CNC-40 based carbon fibers, when carbonization temperature increased from 1000 to 1300 °C, larger crystal sizes ($L_{2\theta \approx 26°}$ and $L_{2\theta \approx 43°}$) and higher plane orientation (f_{002}) are observed, as expected. At 1300 °C carbonization temperature, carbonized PAN/CNC fibers show a relatively larger crystallite size of (10) plane (2.63 – 3.24 nm) as compared to the carbonized PAN fiber (1.98 nm).

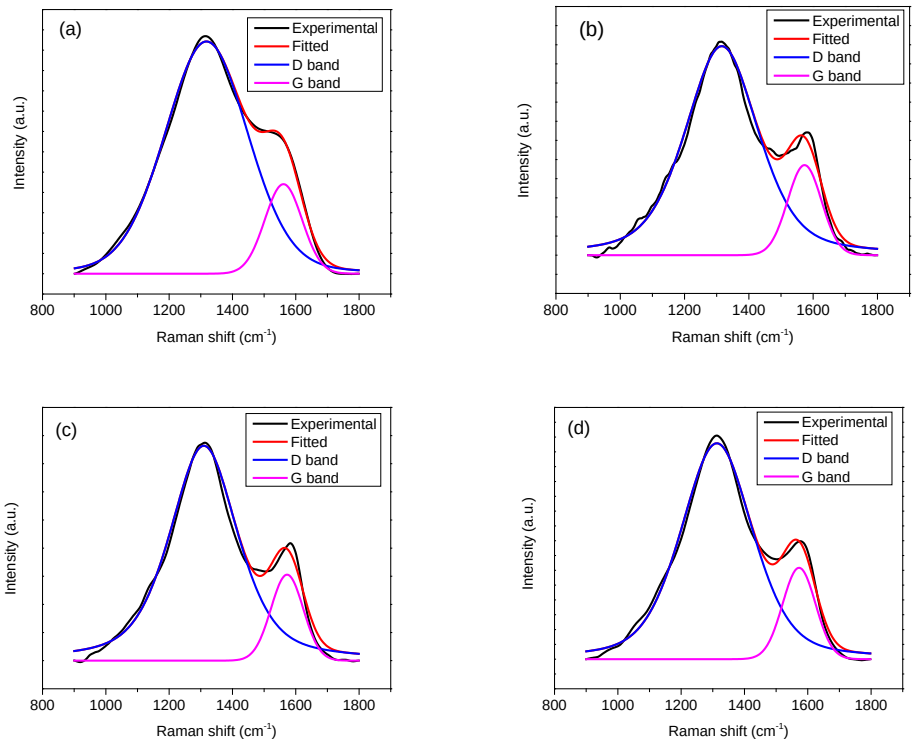

Figure 6. Raman spectra and fitting curves of PAN and PAN/CNC fibers at a draw ratio of 23 carbonized at 1300 °C. (a) PAN, (b) PAN/CNC-10, (c) PAN/CNC-20, (d) PAN/CNC-40.

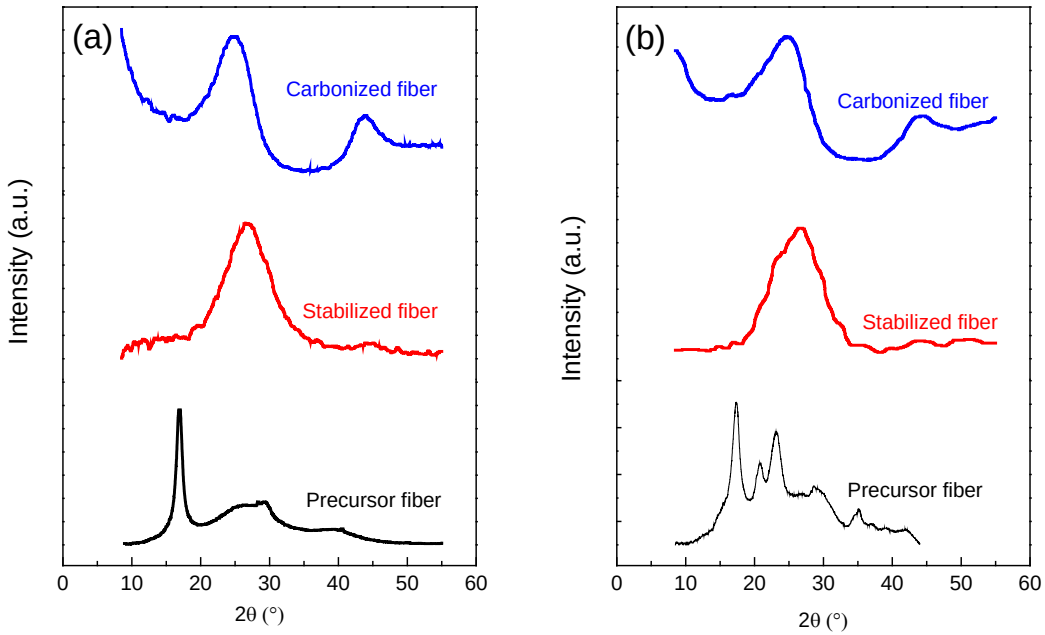

Figure 7. Integrated WAXD scans of precursors, stabilized, and carbonized fibers (at 1000°C) for (a) PAN and (b) PAN/CNC-40.

Table 7. Structural parameters of carbonized PAN and PAN/CNC fibers.

	PAN		PAN/CNC-10	PAN/CNC-20	PAN/CNC-40	
Carbonization Temperature	1000°C	1300°C	1300 °C	1300 °C	1000 °C	1300 °C
$d_{(002)}$ [a] (nm)	0.346	0.356	0.340	0.342	0.355	0.347
$L_{(002)}$ [b] (nm)	1.14	1.36	1.54	1.37	1.15	1.44
$L_{(10)}$ [c] (nm)	1.32	1.98	2.98	3.24	1.94	2.63
f_{002} [d]	0.73	0.75	0.77	0.77	0.74	0.79
Z_{002} [e] (deg)	35.4	33.4	30.8	29.5	33.8	27.2

[a] $d_{(002)}$: *d*-spacing of (002) plane at $2\theta \sim 26°$.
[b] Crystal size of (002) plane at $2\theta \sim 26°$, according to Scherrer's equation with $K = 0.9$
[c] Crystal size of (10) plane at $2\theta \sim 43°$, according to Scherrer's equation with $K = 0.9$
[d] orientation factor of (002) plane
[e] Full-width at half-maximum (FWHM) from azimuthal scans of (002) plane at $2\theta \sim 26°$.

High resolution TEM was used to characterize the microstructure of stabilized and carbonized PAN/CNC-20 fiber. As shown in Figures 8 (a-c), small bright regions with diameters in the range of 10-30 nm are individually distributed in the relatively dark matrix, for the PAN/CNC-20 fibers are stabilized in air. After carbonization, carbon transformed from PAN and CNCs show clear boundary in the carbonized fibers (Figure 8(d-f)). Unlike carbonized PAN/carbon nanotubes fibers, which show graphite templating behavior in the vicinity of carbon nanotubes, carbonized PAN/CNC fibers show a biphasic carbon structure (Figure 8f). Thus a new class of carbon fibers can be made from PAN/CNC.

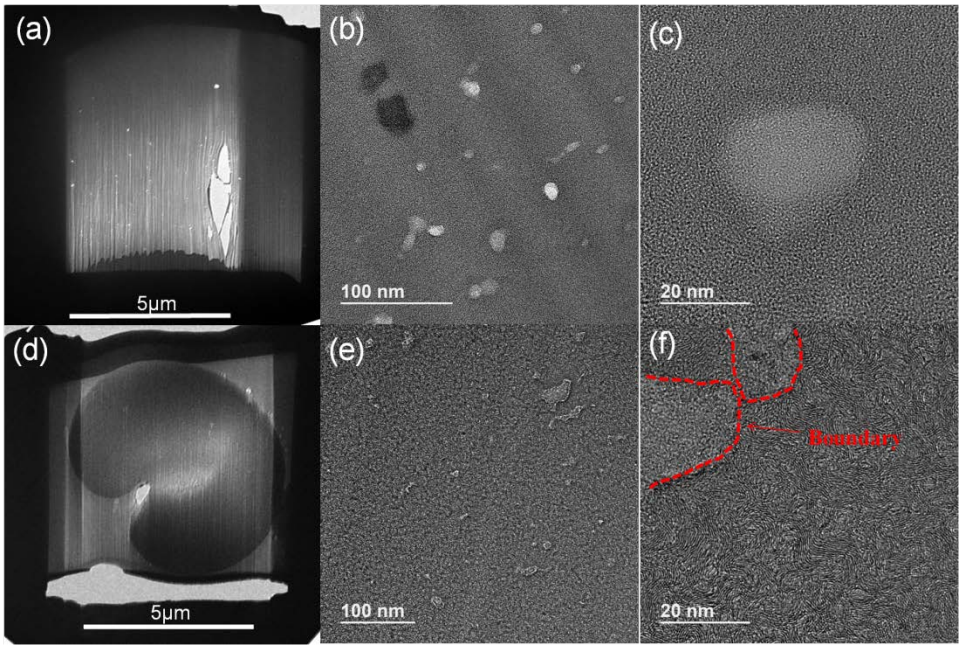

Fig. 8. TEM images of stabilized (a-c) and carbonized (d-f) PAN/CNC-20 fibers.